

Complexity Results on Untangling Planar Rectilinear Red-Blue Matchings

Arun Kumar Das* Sandip Das† Guilherme D. da Fonseca‡ Yan Gerard§
Bastien Rivier¶

Abstract

Given a rectilinear matching between n red points and n blue points in the plane, we consider the problem of obtaining a crossing-free matching through flip operations that replace two crossing segments by two non-crossing ones. We first show that (i) it is NP-hard to α -approximate the shortest flip sequence, for any constant α . Second, we show that when the red points are colinear, (ii) given a matching, a flip sequence of length at most $\binom{n}{2}$ always exists and (iii) the number of flips in any sequence never exceeds $\binom{n}{2} \frac{n+4}{6}$. Finally, we present (iv) a lower bounding flip sequence with roughly $1.5\binom{n}{2}$ flips, which disproves the conjecture that $\binom{n}{2}$, reached in the convex case, is the maximum. The last three results, based on novel analyses, improve the constants of state-of-the-art bounds.

1 Introduction

We consider the problem of untangling a planar rectilinear red-blue matching. We are given a set of $2n$ points in the plane, partitioned into a set R of n red points, and a set B of n blue points, in general position (no three colinear points, unless they have the same color).

A *configuration* is a set of n line segments where each point of R is matched to exactly one point of B , i.e. a perfect rectilinear red-blue matching. A flip is a combinatorial operation changing a configuration into another [7, 16]. In our case, a flip replaces two crossing segments by two non-crossing ones (Figure 1).

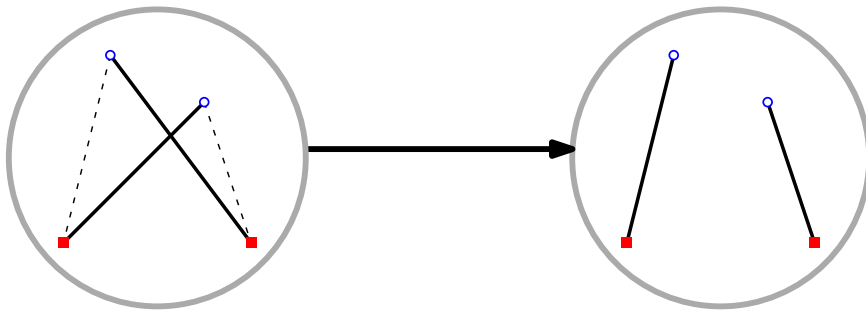


Figure 1: A flip. Red points are represented by solid squares and blue points by hollow circles.

The *reconfiguration graph* of R, B is the directed simple graph whose vertices \mathcal{V} are the configurations, and such that there is a directed edge from a configuration M_1 to another one

*Indian Statistical Institute, Kolkata, India. Email: arund426@gmail.com

†Indian Statistical Institute, Kolkata, India. Email: sandipdas@isical.ac.in

‡Aix-Marseille Université and LIS, France. Email: guilherme.fonseca@lis-lab.fr

§Université Clermont Auvergne and LIMOS, France. Email: yan.gerard@uca.fr

¶Université Clermont Auvergne and LIMOS, France. Email: bastien.rivier@uca.fr

M_2 whenever a flip transforms M_1 into M_2 . Note that the reconfiguration graph is acyclic [6]. Let $\mathcal{S} \subseteq \mathcal{V}$ be the set of sinks, which corresponds to the crossing-free configurations. Given two configurations $u, v \in \mathcal{V}$, let $\mathcal{P}(u, v)$ be the set of directed paths from u to v . Given a path P , let the *length* of P , denoted $|P|$, be the number of edges in P . The *distance* from u to v denoted $d(u, v)$ is the minimum path length from u to v . The *distance* from u to \mathcal{S} , $d(u, \mathcal{S})$, also abbreviated as $d(u)$, is the minimum path length from u to a configuration in \mathcal{S} . We are interested in two parameters of this reconfiguration graph:

$$\mathbf{d}(R, B) = \max_{u \in \mathcal{V}} \min_{v \in \mathcal{S}} \min_{P \in \mathcal{P}(u, v)} |P| \quad \text{and} \quad \mathbf{D}(R, B) = \max_{u \in \mathcal{V}} \max_{v \in \mathcal{S}} \max_{P \in \mathcal{P}(u, v)} |P|.$$

This leads to the definitions of $\mathbf{d}(n)$ and $\mathbf{D}(n)$ respectively as the maximum of $\mathbf{d}(R, B)$ and $\mathbf{D}(R, B)$ with $|R| = |B| = n$. An *untangle sequence* is a path in the reconfiguration graph ending in \mathcal{S} . Intuitively, the value of \mathbf{d} corresponds to the minimum length of an untangle sequence in the worst case, while \mathbf{D} corresponds to the longest untangle sequence.

We also consider a more specific version of the problem where the red points are colinear [4], say, on the x -axis. As the flips on each half-plane defined by the x -axis are independent, we additionally suppose all blue points to lie on the upper half-plane, without loss of generality. The matchings in this case are called *red-on-a-line* matchings.

Related work : The parameters \mathbf{d} , \mathbf{D} have been studied in several different contexts with similar definitions of a flip, but considering other configurations.

In 1981, an $O(n^3)$ upper bound on $\mathbf{D}(n)$ was stated in the context of optimizing a TSP tour [23] (the configurations are polygons). This upper bound should be compared to the exponential lower bound on $\mathbf{D}(n)$ when the flips are not restricted to crossing segments, as long as they decrease the Euclidean length of the tour [10]. The convex case (i.e. the case where the points are in convex position) has been studied in [20, 26].

In the non-bipartite version of the rectilinear perfect matching problem, there are two possible pairs of segments to replace a crossing pair. This additional choice yields an $n^2/2$ upper bound on $\mathbf{d}(n)$ [6].

It is also possible to relax the flip definition to all operations that replace two segments by two others with the same four endpoints, whether they cross or not, and generalize the configurations to multigraphs with the same degree sequence [12, 13, 16]. In this context, finding the shortest path from a given configuration to another in the reconfiguration graph is NP-hard, yet 1.5-approximable [2, 3, 11, 24]. If we additionally require the configurations to be connected graphs, the same problem is NP-hard and 2.5-approximable [8].

Reconfiguration problems in the context of triangulations are widely studied [19]. A flip consists of removing one edge and adding another one while preserving a triangulation. It is known that $\Theta(n^2)$ flips are sufficient and sometimes necessary to obtain a Delaunay triangulation [14, 17]. Determining the flip distance between two triangulations of a point set [18, 21] and between two triangulations of a simple polygon [1] are both NP-hard.

Considering perfect matchings of an arbitrary graph (instead of the complete bipartite graph on R, B), a flip amounts to exchanging the edges in an alternating cycle of length four. It is then PSPACE-complete to decide whether there exists a path from a configuration to another [5]. There is, actually, a wide variety of reconfiguration contexts derived from NP-complete problems where this same accessibility problem is PSPACE-complete [15]. Many other reconfiguration problems are presented in [22].

Getting back to our context of rectilinear red-blue matchings, the values of \mathbf{d} and \mathbf{D} have been determined almost exactly in the convex case (see Table 1). Notice that the $n - 1$ lower bound on $\mathbf{d}(n)$ carries to both the general and red-on-a-line cases [6]. It is notable that the upper bound on $\mathbf{D}(n)$ is also the best known bound on $\mathbf{d}(n)$ and has not been improved since 1981 [23].

Table 1: Lower and upper bounds on $\mathbf{d}(n)$ and $\mathbf{D}(n)$ for red-blue matchings.

	$\mathbf{d}(n)$ bounds		$\mathbf{D}(n)$ bounds	
	lower	upper	lower	upper
general	$1.4n^{(a)}$, Thm. 5.2	$\binom{n}{2}(n-1)$, [6, 23]	$\frac{3}{2}\binom{n}{2} - \frac{n}{4}^{(b)}$, Thm. 5.1	$\binom{n}{2}(n-1)$, [6, 23]
convex	$1.4n^{(a)}$, Thm. 5.2	$2n-2$, [4]	$\binom{n}{2}$, [6]	$\binom{n}{2}$, [4]
red-on-a-line	$n-1$, [6]	$\binom{n}{2}$, Thm. 3.1	$\frac{3}{2}\binom{n}{2} - \frac{n}{4}^{(b)}$, Thm. 5.1	$\binom{n}{2} \frac{n+4}{6}$, Thm. 4.1

^(a) For n multiple of 20.

^(b) For even n .

Contributions. We show in Section 2 that it is NP-hard to α -approximate the shortest untangle sequence starting at a given matching, for any fixed $\alpha \geq 1$.

The following results are summarized in Table 1. An improved lower bound on $d(n)$ in the convex case is presented in Section 5. The remainder of the paper considers the red-on-a-line case. In Section 3, we slightly improve the former $\binom{n+1}{2}$ upper bound on $\mathbf{d}(n)$ [4], using a simpler algorithm and a novel analysis. In Section 4, we asymptotically divide by 6 the historical $\binom{n}{2}(n-1)$ upper bound on $\mathbf{D}(n)$ [6, 23], using a different potential argument.

In Section 5, we present a counter-example to the intuitive conjecture that the longest untangle sequence is attained in the convex case (where the number of crossings is maximal). We take advantage of points that are not in convex position to increase the lower bound by a factor of $\frac{3}{2}$. This red-on-a-line lower bound on $\mathbf{d}(n)$ carries over to the general case (and even to the case of general perfect matchings without color distinction among the points). The weaker conjecture that $\mathbf{D}(n)$ is quadratic [6] still holds, though.

2 NP-Hardness

In this section, we prove the NP-hardness of the following problem.

Problem 1. *Let $\alpha \geq 1$ be a constant.*

Input: M , a red-blue matching.

Output: An untangle sequence starting at M of length at most α times $d(M)$.

We have the following theorem.

Theorem 2.1. *Problem 1 is NP-hard for all $\alpha \geq 1$.*

We reduce the rectilinear planar monotone 3-SAT problem (*RPM 3-SAT*), a known NP-complete problem [9], to Problem 1. An arbitrary gap between the length of the shortest untangle sequences corresponding to accepted and rejected instances of RPM 3-SAT gives the approximation hardness of Problem 1 [25].

2.1 Reduction strategy

In *RPM 3-SAT*, the *graph* of a CNF formula is the bipartite graph with the variables and clauses as vertices, and where there is an edge between a variable and a clause if and only if the clause contains the variable. A CNF formula is *monotone* if each clause contains either only positive or only negative variables. A *rectilinear planar monotone 3-CNF (RPM 3-CNF)* formula is a monotone formula whose graph can be drawn with no intersection, and with the three following conventions (Figure 2). (i) The variables and the clauses are represented by axis-parallel rectangles. (ii) The variable rectangles lie on the x -axis. (iii) The positive clause rectangles are above the x -axis, the negative ones, below. We call such a drawing the *planar embedding* of Φ .

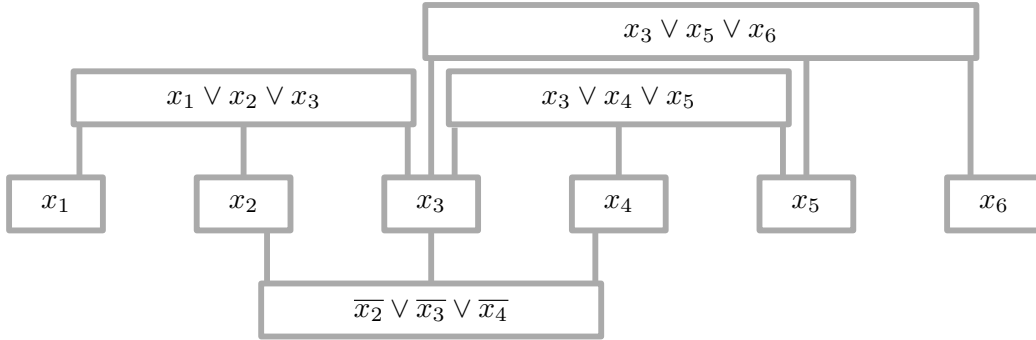


Figure 2: An RPM 3-CNF formula.

The idea of the reduction is that, given an RPM 3-SAT formula Φ , we draw a rectilinear red-blue matching M_Φ of polynomial size such that all the untangle sequences starting at M_Φ are of length at most k_1 if Φ is satisfiable, and of length at least k_2 if Φ is not satisfiable.

The aforesaid matching M_Φ is built upon the planar embedding of Φ . The variable rectangles are replaced by variable gadgets (Figure 3). The clause rectangles together with the corresponding edges are replaced with clause gadgets (Figure 8). A clause gadget consists of two OR gadgets, working like OR gates, and is connected to a padding gadget. If a clause is satisfied, then any untangle sequence of the two OR gadgets will end without creating any crossing in the padding gadget. If a clause is not satisfied, then any untangle sequence of the two OR gadgets will end creating a crossing in the padding gadget, which will trigger an arbitrary long series of flips, thus ensuring an arbitrary gap $k_2 - k_1$.

2.2 Details of the Reduction

The proof of Theorem 2.1 is decomposed into the following lemmas, most of them proven by examining all the possible untangle sequences starting at a given gadget configuration. Each gadget has been designed to have as few untangle sequences as possible, all leading to the same final configuration, except for the variable gadget, which is to have two final configurations.

Variable gadgets. A *variable gadget* is a three-segment configuration built on the four endpoints of an axis-parallel rectangle as follows (Figure 3). The two leftmost endpoints of the rectangle are colored red, the two rightmost ones are colored blue. One of the segments of the matching is the diagonal joining the bottom left red point to the top right blue point. We add one red point on the vertical line splitting the rectangle in two symmetric halves, just above the diagonal, in the inside of the rectangle. This red point is connected to the bottom right blue point. Symmetrically, we add one blue point on the same vertical, just below the diagonal. This blue point is connected to the top left red point.

We will refer to the triangle consisting of the three topmost points of a variable gadget as the *top triangle* of the variable gadget.

Lemma 2.2. *A variable gadget is the starting configuration of exactly two untangle sequences of length 1 ending in distinct configurations.*

Proof. It is straightforward to check the two possible cases. □

We can therefore represent each variable x of a propositional formula by a variable gadget. Assigning x to a truth value amounts to choosing one of the two possible untangle sequences, with the convention that the lower edge of the rectangle is present in the final configuration if $x = 1$ (i.e. x is “true”), and that the upper edge of the rectangle is present if $x = 0$ (Figure 3).

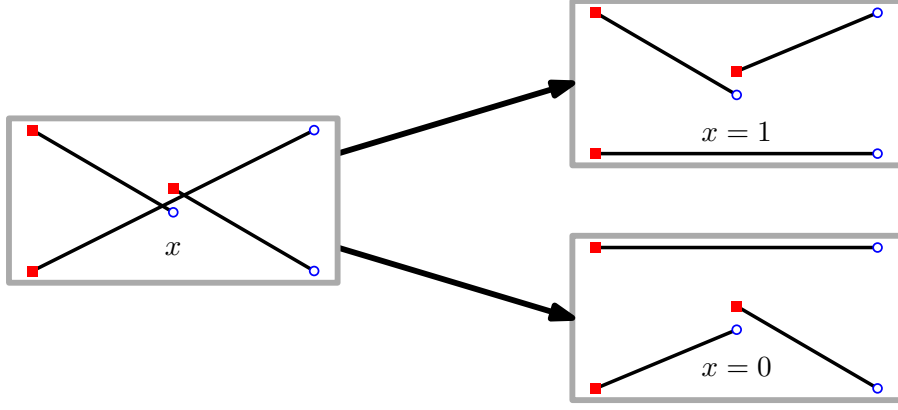


Figure 3: A variable gadget and its two untangle sequences.

OR gadgets. An *OR gadget* consists of four three-segment configurations built on a common point set, say $\{r_1, r_2, r'_2, r_3\}$ for the red points, and $\{b_1, b'_1, b_2, b_3\}$ for the blue points, as follows (see the first configuration in each of Figures 4(a), 4(b), 4(c), and 4(d), ignoring the dashed segments). The $0 \vee 0$ configuration consists of the segments $r_1b'_1, r'_2b_2, r_3b_3$, and only the first two are not crossing. The $0 \vee 1$ configuration consists of the segments $r_1b'_1, r_3b_3, r_2b_2$, and only the first two are crossing. The $1 \vee 0$ configuration consists of the segments r'_2b_2, r_3b_3, r_1b_1 , and only the first two are crossing. The $1 \vee 1$ configuration consists of the segments r_1b_1, r_2b_2, r_3b_3 , and is crossing-free. In addition to these constraints, the point set also satisfies the following ones. The following three configurations are crossing-free: $\{r_1b_2, r'_2b_3, r_3b'_1\}$, $\{r_1b_3, r_2b_2, r_3b'_1\}$, and $\{r_1b_1, r'_2b_3, r_3b_2\}$. In each of the following two configurations, only the first two segments are crossing: $\{r_1b_3, r'_2b_2, r_3b'_1\}$, and $\{r_1b'_1, r_3b_2, r'_2b_3\}$.

Note that, in any of the four configurations of an OR gadget, there is one unused blue point and one unused red point. If the unused blue point is b_1 (respectively b'_1), we say that the *left input* of the OR gadget is 0 (respectively 1). Symmetrically, if the unused red point is r_2 (respectively r'_2), we say that the *right input* of the OR gadget is 0 (respectively 1). To complete the similarity with a logical gate, we also define the *output* of the OR gadget as 0 if the segment r_1b_2 is present in all the final configurations of any untangle sequence starting at the OR gadget's configuration, and as 1 if the segment r_1b_2 is absent of all the same final configurations. The output is undefined otherwise. The following lemma states that the truth table of the logical gate associated with an OR gadget is indeed the one of an OR gate.

We will refer to the smallest of the triangles consisting of the segment r_1b_2 and induced by all the other segments we have mentioned in the definition of an OR gadget as the *top triangle* of the OR gadget. It is the shaded triangle in Figure 4(d).

Lemma 2.3. *The output of an OR gadget is always well defined, and is 0 if and only if the two inputs of the OR gadget are both 0. More precisely, we have the following.*

1. *The $0 \vee 0$ configuration is the starting configuration of exactly two untangle sequences, each of length 2, and ending at the same configuration containing the upper segment r_1b_2 (Figure 4(a)).*
2. *The $0 \vee 1$ configuration is the starting configuration of a unique untangle sequence of length 1 ending at a configuration excluding the upper segment r_1b_2 (Figure 4(b)).*
3. *The $1 \vee 0$ configuration is the starting configuration of a unique untangle sequence of length 1 ending at a configuration excluding the upper segment r_1b_2 (Figure 4(c)).*
4. *The $1 \vee 1$ configuration is already crossing free. It excludes the upper segment r_1b_2 (Figure 4(d)).*

Proof. We consider the four configurations of an OR gadget and all their possible untangle sequences (Figure 4). \square

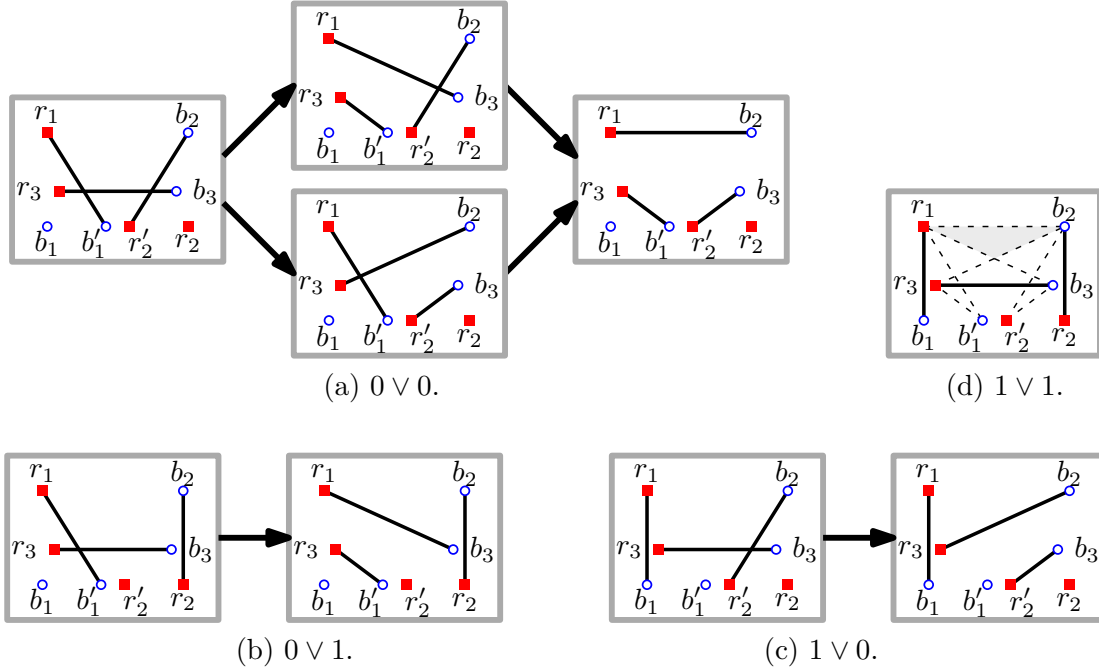


Figure 4: The four configurations of an OR gadget, with their untangle sequences.

Clause gadgets. A *clause gadget* consists of two OR gadgets, the output of the first one being “connected” to the left input of the second one (Figure 5). More precisely, a clause gadget is built on seven red points, say $r_4, r_5, r_6, r_7, r_8, r_{10}, r_{11}$, and six blue points, say $b_4, b_5, b_6, b_7, b_8, b_9$ such that the following maps correspond to two OR gadgets (using the OR gadget previous notations), and such that r_8 lie in the inside of the top triangle of the first OR gadget and is the only overlap between the two OR gadgets.

First OR gadget: $(r_4, b_4, r_5, b_5, r_6, b_6, b_9, r_{10}) \mapsto (r_1, b_1, r_2, b_2, r_3, b_3, b'_1, r'_2)$.

Second OR gadget: $(r_4, b_6, r_7, b_7, r_8, b_8, b_5, r_{11}) \mapsto (r_1, b_1, r_2, b_2, r_3, b_3, b'_1, r'_2)$,

with the exception that the segment $r_6 b_5$ may also play the role of $r_1 b_1$.

Similarly to an OR gadget, a clause gadget consists of 2^3 configurations, namely the $x \vee y \vee z$ configurations with $(x, y, z) \in \{0, 1\}^3$. We define the *left*, *middle*, and *right input* of a clause gadget as the left input of the first OR gadget, the right input of the first OR gadget, and the right input of the second OR gadget. We define the *output* of a clause gadget as the output of the second OR gadget. The following lemma states that the truth table of the logical gate associated with a clause gadget is indeed the expected one.

Lemma 2.4. *The output of a clause gadget is always well defined, and is 0 if and only if the three inputs of the clause gadget are all 0. More precisely, we have the following.*

1. All the untangle sequences starting at the $0 \vee 0 \vee 0$ configuration are of length 4, and they end at the same configuration containing the upper segment $r_4 b_7$.
2. All the untangle sequences starting at each of the $x \vee y \vee z$ configurations, where exactly one of x, y , or z is 1, are of length 2, and they end at the same configuration excluding the upper segment $r_4 b_7$.

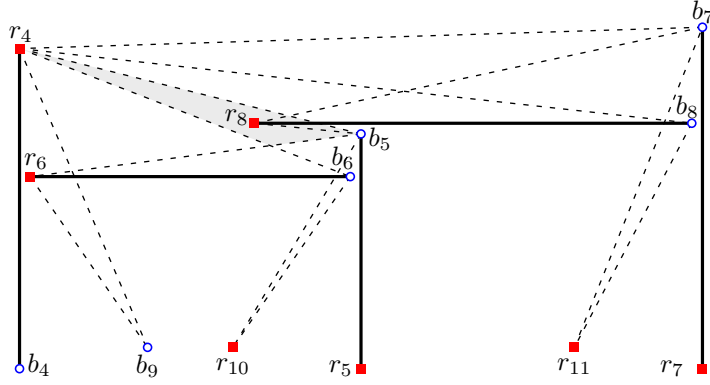


Figure 5: A clause gadget.

3. The unique untangle sequence starting at each of the $x \vee y \vee z$ configurations, where exactly two of x, y , and z are 1, is of length 1, and it ends at a configuration excluding the upper segment $r_4 b_7$.
4. The $1 \vee 1 \vee 1$ configuration is already crossing free, and it excludes the upper segment $r_4 b_7$.

Proof. It is a consequence of Lemmas 2.2 and of the fact that the OR gadgets are connected so as to not interfere. Indeed, by construction, r_8 lie in the inside of the top triangle of the first OR gadget, and is the only overlap between the two OR gadgets. This ensures that all untangle sequences never give rise to an extra crossing that does not already belong to one of the two OR gadgets. In Figure 5, we have drawn with dashed line segments all the possible created segments during any possible untangle sequence. \square

Padding gadgets. Let k be a non-negative integer. A k -padding gadget triggered by the segment s consists of two configurations built by induction as follows. The first configuration, denoted M_k , contains s ($s = r_4 b_7$ in Figure 6) and is called the *triggered configuration* of the padding gadget (s creates a crossing). The second configuration is called the *non-triggered configuration*, and is deduced from the triggered one by removing s (it is crossing free). If $k = 0$, then the triggered configuration of a k -padding gadget consists of only the segment s . If $k \geq 1$, then the triggered configuration of a k -padding gadget consists of M_{k-1} , the triggered configuration of a $(k - 1)$ -padding gadget, to which we add one new segment crossing only the last created segment of the only untangle sequence starting at M_{k-1} (Figure 6, the dashed segments are all the possible created segments in the unique untangle sequence).

Lemma 2.5. *Let k be a non-negative integer. There is a unique untangle sequence starting at the triggered configuration of a padding gadget, and it is of length k . The non-triggered configuration of a padding gadget is already crossing free.*

Proof. The definition of a k -padding gadget yields Lemma 2.5. \square

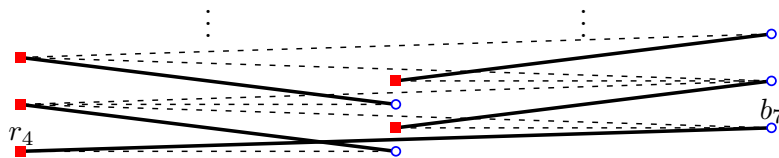


Figure 6: The triggered configuration of a padding gadget.

We complete each clause gadget with a padding gadget in order to penalize a non-satisfied clause by an arbitrary long untangle sequence (Figure 7). Notice that a clause gadget with

padding can be arbitrarily scaled and that the position of a clause rectangle is only constrained by the planar embedding of Φ .

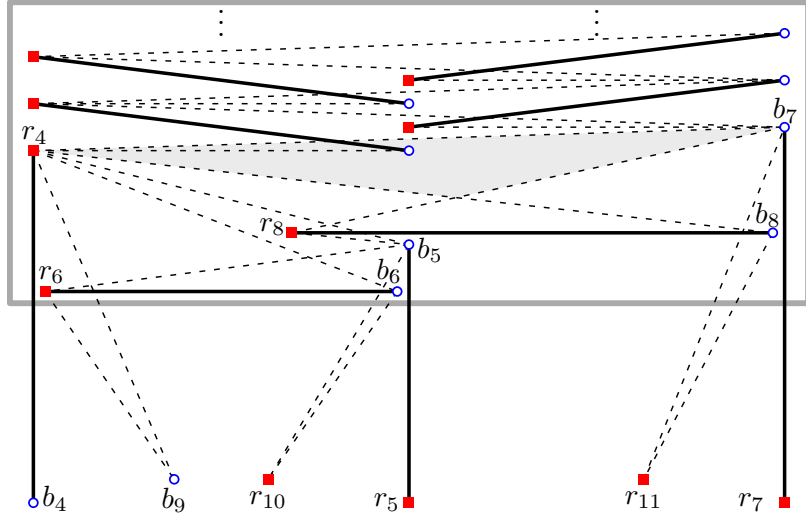


Figure 7: A clause gadget connected to a padding gadget.

Branching. The connections of the variables gadgets require a particular attention. First note that there is a one-to-one correspondence between the vertical edges of the planar embedding of Φ and the vertical segments of M_Φ , and that we stop making the distinction. In the following, we study the possible configurations of such connections, eventually reaching the definition of a *branching configuration* and an associated lemma.

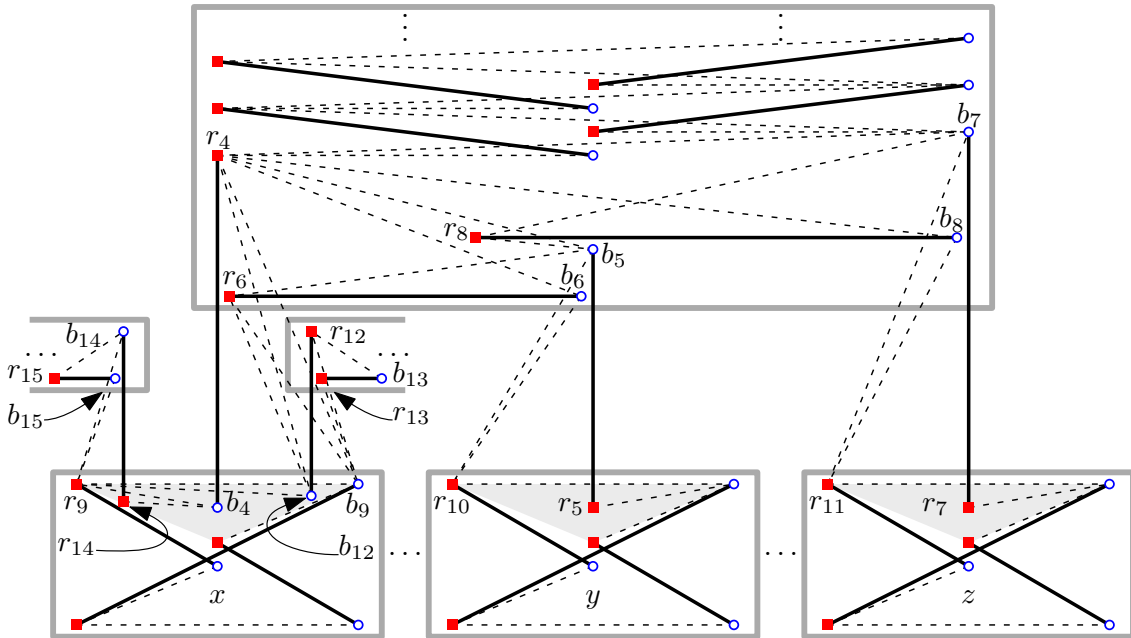


Figure 8: A clause gadget with padding connected to its variable gadgets, with branching on x .

In the planar embedding of Φ , each variable is adjacent to vertical edges from several clauses. Without loss of generality, we only consider positive clauses. We partition these vertical edges in three classes:

1. A *left edge* is the leftmost vertical edge of a (positive) clause (e.g. r_4b_4 in Figure 8). According to the definition of a clause gadget, a left edge is connected to a variable with a blue point added in the upper triangle of the variable gadget.
2. A *middle edge* is the middle vertical edge of a clause (e.g. r_5b_5 in Figure 8). A middle edge is connected to a variable with a red point added in the upper triangle of the variable gadget, and will actually play the same role as a right edge.
3. A *right edge* is the rightmost vertical edge of a clause (e.g. r_7b_7 in Figure 8). A right edge is connected to a variable with a red point added in the upper triangle of the variable gadget.

We additionally define the *top vertical points* as the topmost endpoints of the vertical segments of the positive clause gadgets of M_Φ (e.g. $b_{14}, r_4, r_{12}, b_5, b_7$ in Figure 8). Similarly, the *bottom vertical points* are the bottom endpoints of the same vertical segments (e.g. $r_{14}, b_4, b_{12}, r_5, r_7$ in Figure 8). Finally, we define the *substitute* point of a top vertical point p as the point lying in the corner of the same clause gadget just below p (e.g. r_6 is the substitute of r_4 in Figure 9(c)).

The vertical edges connected to a variable, ordered from left to right, are firstly right edges with an increasing height, then, at most one middle edge with the maximum height, and finally, left edges with a decreasing height. It follows that the corresponding top vertical points are in convex position, and that they are, from left to right, a certain number of blue points, say a , followed by a certain number of red points, say b .

As for the bottom vertical points, we adjust their height so that they also reach a convex position (e.g. the points r_{14}, b_4 , and b_{12} in Figure 9). We finally adjust the horizontal position of the substitute points so as to have their corresponding segment crossing as few potentially-created segments (the dashed segments in Figure 9) as possible, without breaking the clause gadget (e.g. in Figure 9, segment $r_{13}b_{13}$ does not cross r_4b_9 , but it has to cross $r_{12}b_9$).

The set of the $2(a + b) + 1$ aforementioned segments is called a *branching configuration* with parameters a, b (such as drawn in Figure 9(b) with plain segments). These configurations have the following property.

Lemma 2.6. *All the untangle sequences starting at a branching configuration with parameters a, b have length $2(a + b)$ and end at the same crossing-free configuration (such as drawn in Figure 9(b)).*

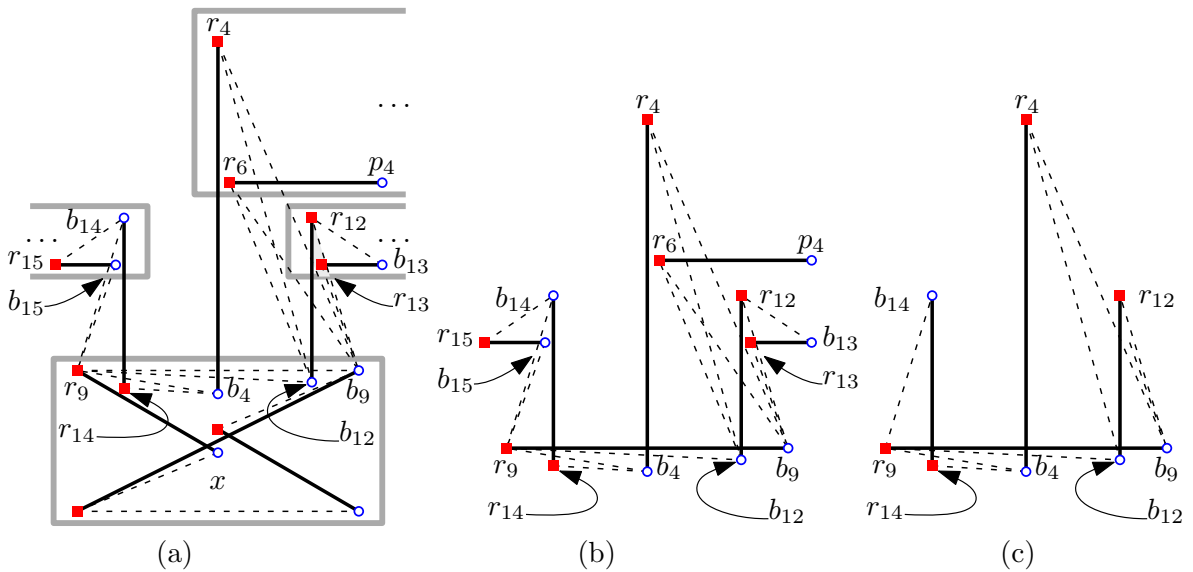


Figure 9: Three views of a branching configuration.

Proof. First note that a simplified version of this result has been proven in [6]. This simplified version amounts to forget all the horizontal segments, except the top segment of the variable gadget (Figure 9(c)).

It is useful to start proving this simplified version before Lemma 2.6. We do an induction on $a + b$. The base case is trivial, but it provides the possible positions of created segments in the untangle sequences (the dashed segments in Figure 9(c)). The inductive case amounts to the following fact. After any flip, the two created segments can play the role of the initial horizontal segment, and induction hypothesis applies on both right and left sub-matching whose convex hulls are now disjoint.

We now address the issue where each vertical segment is paired with a horizontal segment. Recall we have adjusted the positions of each substitute point so that its segment crosses as few potentially-created segments as possible. This ensures that each substitute point can play the role of its corresponding top vertical point from whenever the corresponding horizontal segment has been flipped in an untangle sequence. \square

Matching computation. We have the following lemma.

Lemma 2.7. *Let Φ be an instance of RPM 3-SAT with c clauses and v variables. Let k be a non-negative integer, polynomial in c and v . The matching M_Φ with k -padding gadgets is computed in polynomial time in c and v .*

Proof. Given a planar embedding of Φ , we compute the matching M_Φ with the following algorithm:

1. Put a clause gadget with a k -padding gadget in each clause rectangle and a variable gadget in each variable rectangle, with appropriate scaling.
2. Connect each clause gadget to its corresponding three variable gadgets with the three vertical segments of the clause gadget aligned with the corresponding vertical edges of the planar embedding of Φ .
3. Adjust the vertical position of the bottom vertical points in the top triangle of each variable gadget so as to put them in convex position.
4. Adjust the horizontal position of the substitute points so as to have their corresponding segments cross as few potentially-created segments.

The number of operations in any execution of this algorithm is linear in c and v . \square

Result. The RPM 3-SAT instance being encoded in the matching M_Φ , we have the property that the shortest untangling sequence of M_Φ is short if the instance Φ is satisfiable, and long otherwise.

Lemma 2.8. *We have the following case distinction.*

- Φ is satisfiable if and only if no padding gadget is triggered, in which case $d(M_\Phi)$ is at most $v + 5c$.
- Φ is not satisfiable if and only if at least one padding gadget is triggered, in which case $d(M_\Phi)$ is at least $v + 7 + k$ where k is arbitrarily large.

Proof. It is consequence of Lemmas 2.2, 2.4, 2.5 and 2.6, as we examine the longest and the shortest possible untangle sequences of M_Φ . In any case, v flips will be performed, one per variable (Lemma 2.2).

In the case where no padding gadget is triggered, the length of the longest possible untangle sequences starting at a clause gadget connected to three variable gadgets is 5, and is obtained

by adding 3, the length of the untangle sequences of a $0 \vee 0 \vee 1$ configuration, and 2, for the two connections to the negative variables. Counting 5 flips per clause yields $v + 5c$.

If at least one padding gadget is triggered, this very padding gadget generates k flips. In this case, the length of the shortest possible untangle sequences starting at a clause gadget connected to three variable gadgets and which is known to trigger its padding gadget is 7, and is obtained by adding 4, the length of the untangle sequences of a $0 \vee 0 \vee 0$ configuration, and 3, for the three connections to the negative variables. All the other clause gadgets may be in their $1 \vee 1 \vee 1$ configuration, adding no flip to the shortest untangle sequence, the length of which is thus $v + 7 + k$. \square

We now prove Theorem 2.1, reducing RPM 3-SAT to Problem 1. Let Φ be an instance of RPM 3-SAT with c clauses and v variables. We build the matching M_Φ , which serves as an instance of Problem 1, choosing $k = 5c - 6 + (\alpha - 1)(v + 5c)$. As k is polynomial in the size of the input (α is a constant), the computation of the matching M_Φ is polynomial (Lemma 2.7).

By hypothesis, we compute an untangle sequence starting at M_Φ of length ℓ at most $\alpha d(M_\Phi)$. We decide that Φ is satisfiable if $\ell \leq \alpha(v + 5c)$, and that Φ is not satisfiable if $\ell > \alpha(v + 5c)$.

Indeed, Lemma 2.8 ensures the following. If Φ is satisfiable, the length of the shortest untangle sequence of M_Φ is at most $v + 5c$. Otherwise the length of the shortest sequence is at least $v + 7 + k = \alpha(v + 5c) + 1$. This ends the reduction, and proves Theorem 2.1.

3 Upper Bound on $d(n)$

In this section, we first give some insight into the proof of the following upper bound.

Theorem 3.1. *In the red-on-a-line case, $d(n) \leq \binom{n}{2}$.*

The proof consists of the analysis of the number of flips performed by the following recursive algorithm. We assume general position (no two blue points at same height). Let the *top* segment of a red-on-a-line matching be the segment with the topmost blue endpoint.

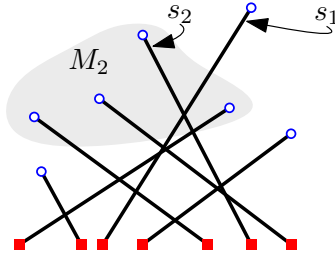


Figure 10: Definitions used in Algorithm 1.

Algorithm 1:

Input : M , a red-on-a-line matching.

Output : An untangle sequence starting at M .

- 0 If $R = B = \emptyset$, then stop.
 - 1 Let M_2 be the set of segments crossing s_1 , the top segment of M (Figure 10). If M_2 is not empty, flip s_1 and s_2 , the top segment of M_2 , and repeat Step 0.
 - 2 Recursively call the algorithm on the sub-matchings on both sides of the updated top segment of M .
-

The idea behind Algorithm 1 stems from the following observations. We define three states for a pair of segments: state **X**, when the segments are crossing, state **H**, when the segments are

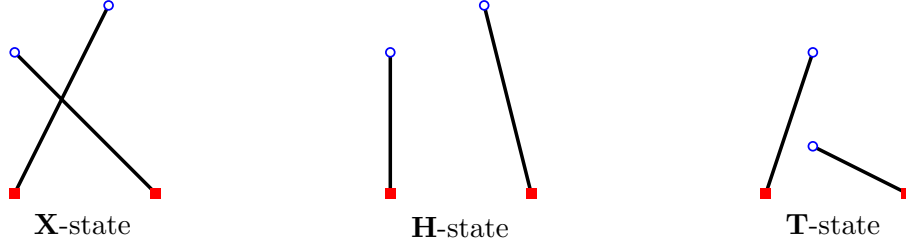


Figure 11: The three different states of pairs of segments.

not crossing and their endpoints are in convex position, and state **T**, when the endpoints are not in convex position (Figure 11). In the convex case, a flip increases the number of **H**-pairs by at least 1, providing the $\binom{n}{2}$ upper bound on $\mathbf{D}(n)$. However, the number of **H**-pairs may decrease in the general case. Figure 12 shows two such situations where there is one **H**-pair involving the segment s before the flip, and none after the flip. Algorithm 1 avoids these situations by choosing to flip top segments. The full proof involves state tracking, a novel approach to analyse flip sequences.

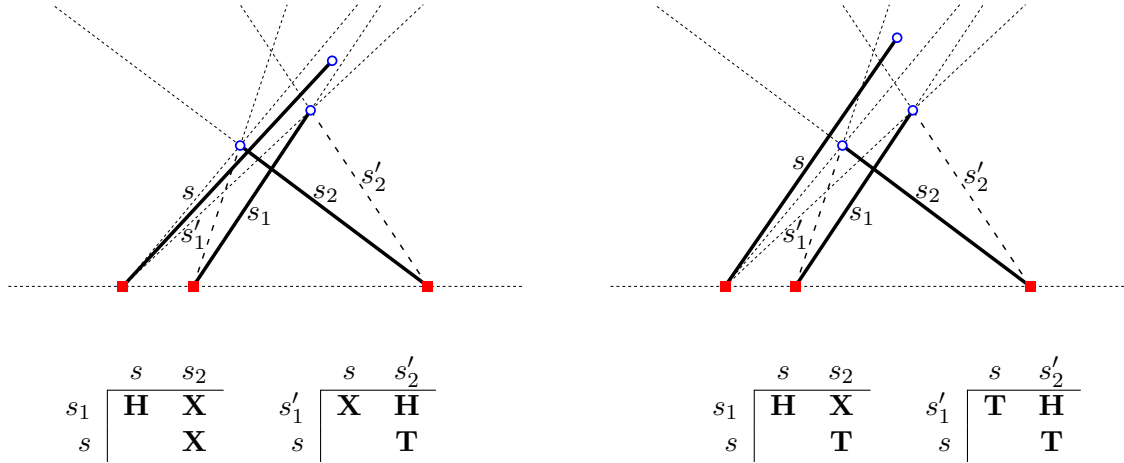


Figure 12: Two cases where the number of **H**-pairs decreases. The flipped pair is s_1, s_2 .

3.1 Proof of Theorem 3.1

In this section, we prove Theorem 3.1. The next three lemmas prove the correctness of Algorithm 1.

Lemma 3.2 ([6]). *If a matching admits a partition of submatchings whose convex hulls are all disjoint, then, any sequence of flips in one of the submatchings never affects the other submatchings (Figure 13).*

Proof. The flip operation leaves the convex hull unchanged (in Figure 13, the dashed segments are the results of possible flip sequences). □

We say that a segment s is *free* if the matching admits a partition of submatchings whose convex hulls are all disjoint, and one of the submatchings consists of the segment s alone. In Figure 13, the segment s is the only free segment.

Lemma 3.3. *Algorithm 1 always frees the top segment before recursive calls (i.e. before step 1).*

Proof. It is easy to follow that the recursive calls of Algorithm 1 happen only when the top segment is free. □

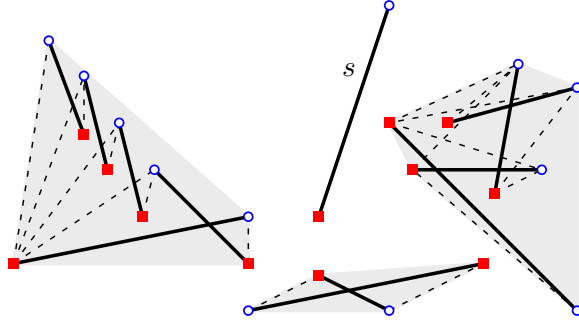


Figure 13: A matching admitting a partition of 4 submatchings whose convex hulls are all disjoint.

Lemma 3.4. *Algorithm 1 is correct.*

Proof. Lemma 3.4 follows from Lemma 3.2 and 3.3. □

In the following, we present a novel approach to analyse flip sequences.

State tracking. As we have seen in Section 3, there are three possible states for a pair of segments: **X**, **H**, and **T** (Figure 11). Given M , a perfect matching of n segments, we choose a one-to-one map between the $\binom{n}{2}$ pairs of segments of M and the integers from 1 to $\binom{n}{2}$. This map will be seen as a vector, indexed from 1 to $\binom{n}{2}$, and will be referred to as a *state vector* of M .

Consider a flip that changes a pair of segments $\{s_1, s_2\}$ into $\{s'_1, s'_2\}$. Let M' denote the resulting matching after the flip. We note that there are three types of pairs of segments in M : the *unaffected* pairs, the *flipped* pair (i.e. $\{s_1, s_2\}$, see Figure 14), and the *affected* pairs (involving exactly one of the two segments s_1 or s_2). Again, we choose a one-to-one map between the $\binom{n}{2}$ pairs of segments of M' and the integers from 1 to $\binom{n}{2}$, in a way that is “consistent” with the former choice in the following sense. We choose the same index for an unaffected pair. We choose the same index as $\{s_1, s_2\}$ for $\{s'_1, s'_2\}$.

As for the affected pairs, we group them by two. Let s be a segment of M distinct from s_1 and s_2 . Let i_1 and i_2 be the indices of $\{s_1, s\}$ and $\{s, s_2\}$, and let \mathbf{S}_1 and \mathbf{S}_2 be their respective states. Let \mathbf{S}'_1 and \mathbf{S}'_2 be the respective states of $\{s'_1, s\}$ and $\{s, s'_2\}$. It is natural to restrict our choice to the following two options.

- Either we choose $\{s'_1, s\}$ to be indexed with i_1 , and $\{s, s'_2\}$ to be indexed with i_2 , in which case we say that the endpoint common to s_1 and s'_1 , and that the endpoint common to s_2 and s'_2 (i.e. the red points in Figure 14) are *preserved*,
- or, conversely, we choose $\{s'_1, s\}$ to be indexed with i_2 , and $\{s, s'_2\}$ to be indexed with i_1 , in which case we say that the endpoint common to s_1 and s'_2 , and that the endpoint common to s_2 and s'_1 (i.e. the blue points in Figure 14) are *preserved*.

The idea is to choose the option that best “tracks” the states of the two pairs. We call such a choice a *tracking choice*, and we say the pairs $\{s_1, s\}$ and $\{s, s_2\}$ are *twins*.

A path in the reconfiguration graph together with a sequence of tracking choices yields a matrix whose j -th line is the state vector of the j -th matching of the path (starting at the 0-th line). Such a matrix will be referred to as a *state matrix*. A column of a state matrix will be seen as the sequence of the states of the pair of segments composing the column. Within such a column, there are 3^2 possible *transitions* from a cell to the next one: $\mathbf{S} \rightarrow \mathbf{S}'$ for $(\mathbf{S}, \mathbf{S}') \in \{\mathbf{X}, \mathbf{H}, \mathbf{T}\}$. We also write $\mathbf{S}_1, \mathbf{S}_2 \rightarrow \mathbf{S}'_1, \mathbf{S}'_2$ when the tracking choice of the twin affected pairs $\{s_1, s\}$ and $\{s, s_2\}$ has yet to be specified. We will use this notation in Figures 14, 15, and 17.

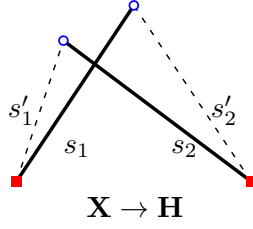


Figure 14: The flipped pair and the corresponding transition.

Lemma 3.5. *It is always possible to make tracking choices that avoid $\mathbf{H} \rightarrow \mathbf{X}$ transitions.*

This lemma actually holds for any rectilinear perfect matching, without any color distinction among the points.

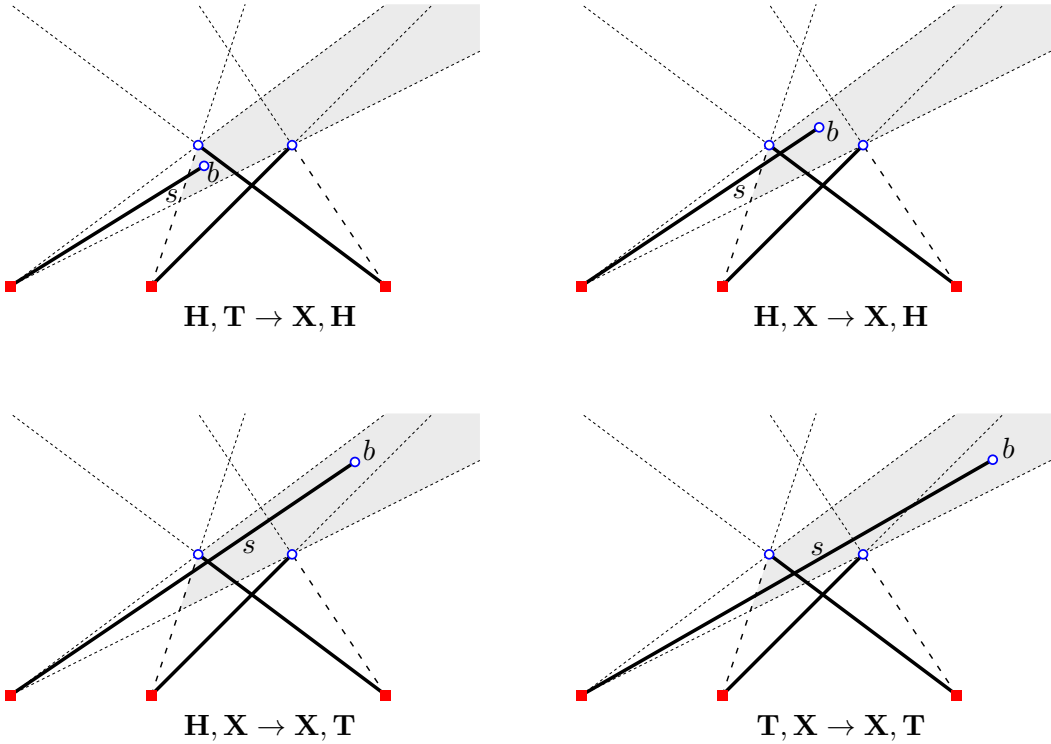


Figure 15: Four critical cases where we can make the tracking choice so as to avoid $\mathbf{H} \rightarrow \mathbf{X}$.

Proof. We consider a flip changing the pair $\{s_1, s_2\}$ into $\{s'_1, s'_2\}$, together with a segment s unaffected by the flip (see Figure 14 for the notations). Without loss of generality, we suppose that $\{s'_1, s\}$ is an \mathbf{X} -pair, and that $\{s_1, s\}$ is an \mathbf{H} -pair. As a consequence, \mathbf{S}_2 , the state of $\{s, s_2\}$, is not \mathbf{H} . Similarly, \mathbf{S}'_2 , the state of $\{s, s'_2\}$, is not \mathbf{X} . Figure 15 shows the four possible configurations. We can see that b , the blue endpoint of s , must lie in the shaded region.

It is, thus, possible to make the tracking choice, where $\{s_1, s\}$ is \mathbf{H} and becomes \mathbf{S}'_2 as $\{s, s'_2\}$, and $\{s, s_2\}$ is \mathbf{S}_2 and becomes \mathbf{X} as $\{s'_1, s\}$. \square

State tracking in the convex case. State tracking also applies to the widely studied convex case, providing a more conceptual proof of the following theorem. Even though we will not use this well-known result, we may as well state it.

Theorem 3.6 ([4]). *In the convex case, any untangle sequence is of length at most $\binom{n}{2}$.*

Again, this theorem actually holds for any rectilinear perfect matching, without any color distinction among the points.

Proof. In the convex case, the \mathbf{T} -state does not exist. Lemma 3.5 thus ensures that the number of \mathbf{H} -pairs increases of at least 1 unit at each flip. \square

State tracking in the red-on-a-line case. There is a lemma, similar to Lemma 3.5, to avoid $\mathbf{H} \rightarrow \mathbf{T}$ transitions. This lemma is weaker, and specific to red-on-a-line matchings. To state it, we define the *upper cone* of two segments r_1b and r_2b as the open affine convex cone with the common blue point b as its origin, and generated by the vectors $\overrightarrow{r_1b}$ and $\overrightarrow{r_2b}$ (Figure 16(a)). We will also use the *upper ray* of a segment as the open ray with the blue point as its origin, the segment as its direction, and going upwards (Figure 16(b)).

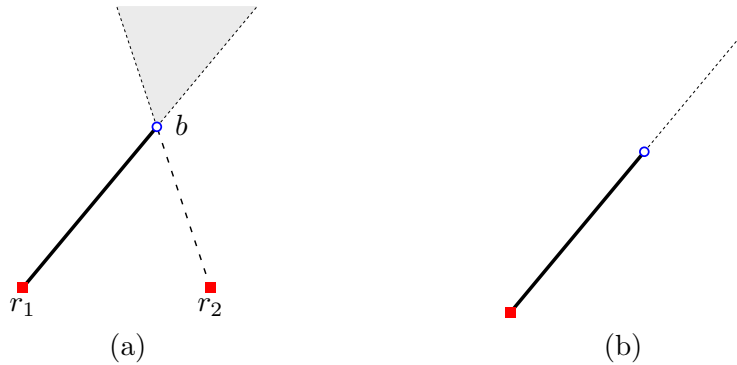


Figure 16: (a) The upper cone of r_1b and r_2b . (b) The upper ray of the segment is dotted.

Lemma 3.7. *It is always possible to make tracking choices so as to avoid transition $\mathbf{H} \rightarrow \mathbf{T}$ for the pairs $\{s_1, s\}$ and $\{s, s_2\}$, except when the blue point b of s is at least in one of the two upper cones of the segments s_1, s_2, s'_1, s'_2 .*

Proof. First, we check that there are only two possible upper cones define by two segments of s_1, s_2, s'_1, s'_2 . Indeed, only two pairs among them have a common blue point.

Then, we note that, for $\{s_1, s\}$ or $\{s, s_2\}$ to be in state \mathbf{H} , the red point r of s cannot be between r_1 and r_2 , the red points of s_1 and s_2 . Without loss of generality, we assume r to lie on the left side of r_1 and r_2 .

For $\{s, s'_1\}$ or $\{s, s'_2\}$ to be in state \mathbf{T} , s has to cross one of the upper rays of s'_1 or s'_2 .

The only two combinations of states for $\{\{s, s_1\}, \{s, s_2\}\}$ and $\{\{s, s'_1\}, \{s, s'_2\}\}$ which do not leave us the choice to avoid the $\mathbf{H} \rightarrow \mathbf{T}$ transition are $\{\mathbf{H}, \mathbf{T}\}$ and $\{\mathbf{T}, \mathbf{T}\}$, and $\{\mathbf{H}, \mathbf{X}\}$ and $\{\mathbf{T}, \mathbf{X}\}$; in both cases, b must be in the right most of the two upper cones of segments s_1, s_2, s'_1, s'_2 (Figure 17). The other cases are either not feasible geometrically, or with a possibility to make tracking choices so as to avoid transition $\mathbf{H} \rightarrow \mathbf{T}$. \square

State tracking for Algorithm 1. We are now in position to prove two final lemmas specific to Algorithm 1, from which Theorem 3.1 follows.

Lemma 3.8. *There exists a sequence of tracking choices to build a state matrix for any execution of Algorithm 1 such that there is at most one transition $\mathbf{X} \rightarrow \mathbf{H}$ per column.*

Proof. We choose a coherent tracking as described above, and reuse the same notations.

Once a segment is free, all the pairs involving it are not, and will never be in state \mathbf{X} (Lemma 3.2).

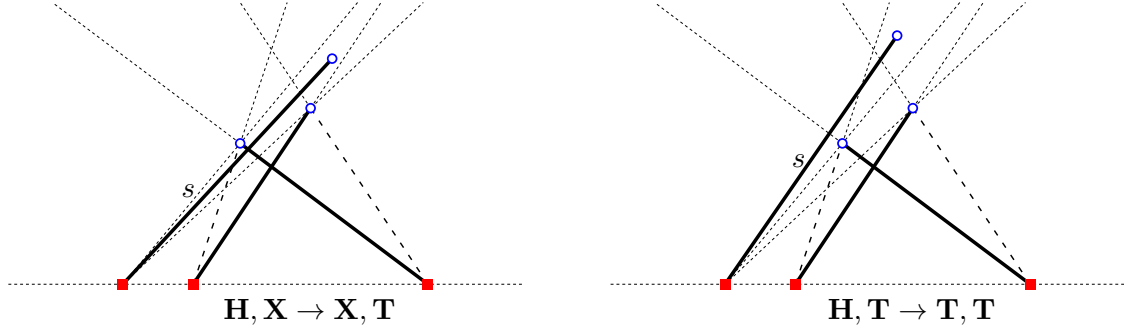


Figure 17: Two cases where tracking choice cannot avoid the transition $\mathbf{H} \rightarrow \mathbf{T}$.

Before one of its two segments is free, the only way a pair could leave state \mathbf{H} is when it is an affected pair $\{s, s_i\}$ ($i = 1$ or 2), and it undergoes transition $\mathbf{H} \rightarrow \mathbf{T}$ (Lemma 3.5). This transition is impossible to avoid by tracking choice only if the blue point of s is higher than the blue point of s_i (Lemma 3.7).

This situation is excluded by Algorithm 1, as only top segments are flipped. \square

Lemma 3.9. *Algorithm 1 performs at most $\binom{n}{2}$ flips.*

Proof. Each flip induces a transition $\mathbf{X} \rightarrow \mathbf{H}$ and a new line in any matrix of any execution of Algorithm 1. It follows from Lemma 3.8 that there are no more lines than there are columns (0-th line aside). As there are $\binom{n}{2}$ columns (the number of pairs of segments in a matching), we conclude that $\binom{n}{2}$ is also the upper bound for the number of flips. \square

Theorem 3.1 follows from Lemma 3.9.

4 Upper Bound on $\mathbf{D}(n)$

In this section we prove the following theorem.

Theorem 4.1. *In the red-on-a-line case, $\mathbf{D}(n) \leq \binom{n}{2} \frac{n+4}{6}$.*

To prove Theorem 4.1, we define a potential function Φ that maps a red-on-a-line matching to an integer from 0 to $\binom{n}{2} \frac{n+4}{3}$. Since this function decreases of at least 2 units at each flip, the theorem follows. We first give the definitions needed to define Φ , together with some insight of the proof.

Let M be a red-on-a-line matching. Let r_1, \dots, r_n be the red points, from left to right. Let ℓ be a line, parallel to the line of the red points and above them. For each k in $\{1, \dots, n\}$, we project the blue points onto ℓ , using r_k as a focal point. Each blue point b is then transformed into $p^k(b)$, the intersection between the ray $r_k b$ and the line ℓ (Figure 18(a)).

We say a pair of segments $\{r_i b, r_j b'\}$, also abbreviated as $\{i, j\}$, is a k -pair when $i \leq k \leq j$. We say a pair of segments $\{r_i b, r_j b'\}$ is k -crossing when the segments $r_i p^k(b)$ and $r_j p^k(b')$ cross (Figure 18(b)). A k -flip is then a flip of a k -pair. We have the following lemma.

Lemma 4.2. *A crossing k -pair is necessarily k -crossing.*

Proof. Let $\{r_i b, r_j b'\}$ be a crossing k -pair. We suppose, without loss of generality, that $i < j$.

The fact that the k -pair $\{r_i b, r_j b'\}$ is crossing means that the four points are in convex position, and that they appear as r_i, r_j, b, b' on their convex hull in counter-clock-wise order. Since $i \leq k \leq j$, the point r_k is also on the convex hull of the four points. Therefore, the projection p^k will not change the convex-hull order and the segments $r_i p^k(b)$ and $r_j p^k(b')$ will cross. \square

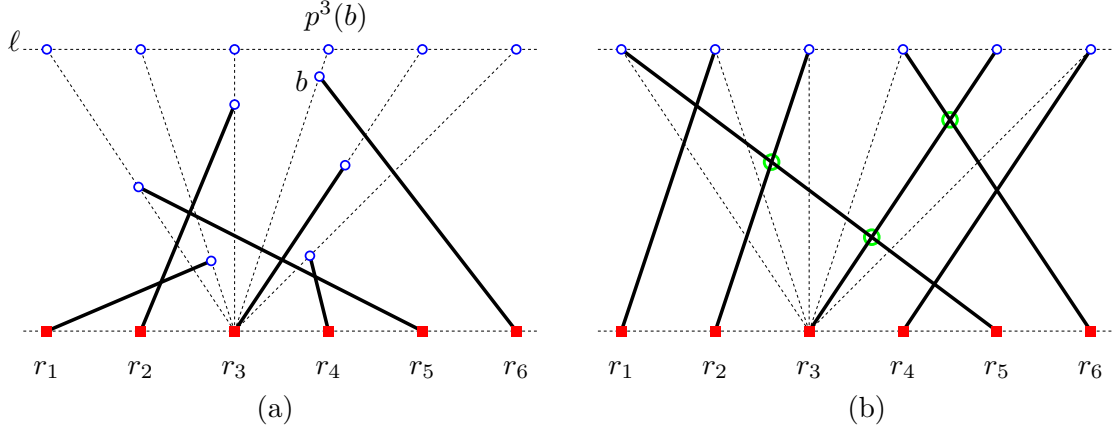


Figure 18: (a) The projection p^k for $k = 3$. (b) The three 3-crossing 3-pairs are circled.

We define $\Phi^k(M)$, the k -th potential of M , as the number of k -crossing k -pairs (Figure 18(b)). Lemma 4.3 shows that the k -th potential Φ^k is at most $(k-1)(n-k) + n - 1$. Lemma 4.4 shows that Φ^k never increases, and decreases of at least 1 unit at each k -flip.

Lemma 4.3. *The k -th potential Φ^k takes integer values from 0 to $-k^2 + k(n+1) - 1$.*

Proof. The k -th potential Φ^k is at most the number of k -pairs. Notice that (i) there are $(k-1)(n-k)$ pairs of the form $\{i, j\}$ with $i < k < j$. (ii) there are $k-1$ pairs of the form $\{i, k\}$ with $i < k$. (iii) and there are $n-k$ pairs of the form $\{k, j\}$ with $k < j$. In total, there are $(k-1)(n-k) + k-1 + n-k$ k -pairs. \square

Lemma 4.4. *The k -th potential Φ^k never increases, and decreases of at least 1 unit at each k -flip.*

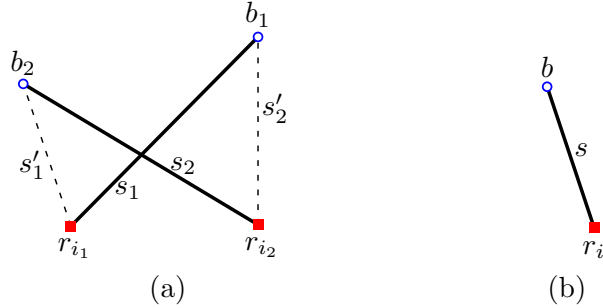


Figure 19: (a) The notations for the flipped pair. (b) The notations for segment s .

Proof. We will track the states in each projection, where the points are in convex position. We fix an arbitrary k . A k -flipped pair necessarily decrements the value of Φ^k of 1 unit. We now prove that the k -th potential Φ^k never increases.

The following four sentences define notations which are summarized in Figure 19. We consider a flip changing the pair $\{s_1, s_2\}$ into $\{s'_1, s'_2\}$, together with a segment s unaffected by the flip. Let i_1, i_2, i be the respective indices of the red endpoints of the segments s_1, s_2, s . Let b_1, b_2, b be the respective blue endpoints of the segments s_1, s_2, s . We suppose that $s'_1 = r_{i_1}b_2$, and $s'_2 = r_{i_2}b_1$.

We treat all the possible cases, from case 1.1 to case 1.3, and from case 2.1 to case 2.2. Each case is subdivided into three sub-cases:

- the sub-case (a) where $p^k(b)$ lie on the left side of $p^k(b_1)$ and $p^k(b_2)$,

- the sub-case (b) where $p^k(b)$ lie in between $p^k(b_1)$ and $p^k(b_2)$, and
- the sub-case (c) where $p^k(b)$ lie on the right side of $p^k(b_1)$ and $p^k(b_2)$.

In each case, we prove that the following four statements holds.

If $\{s, s_2\}$ is not a k -pair, and if $\{s_1, s\}$ is a k -pair which is not k -crossing, then $\{s, s'_1\}$ is not k -crossing either. (1)

If $\{s_1, s\}$ is not a k -pair, and if $\{s, s_2\}$ is a k -pair which is not k -crossing, then $\{s, s'_2\}$ is not k -crossing either. (2)

If both $\{s, s_2\}$ and $\{s_1, s\}$ are k -pair, exactly one of which is not k -crossing, then at least one of $\{s'_1, s\}$ or $\{s, s'_2\}$ is not k -crossing. (3)

If both $\{s, s_2\}$ and $\{s_1, s\}$ are k -pair, and both are not k -crossing, then both $\{s'_1, s\}$ and $\{s, s'_2\}$ are not k -crossing. (4)

The fact that the k -th potential Φ^k never increases will stand as a consequence of these four statements. Of course, in a given situation, at most one of the four statements is not empty. One may have noted the symmetry of statements (1) and (2). In fact, we will not consider statement (2) thanks to symmetry considerations. One may have also noted that statements (3) and (4) amount to Lemma 3.5 in the convex case (i.e. no \mathbf{T} -state), provided the flip pair is k -crossing. We will prove this statements again regardless.

Case 1: the flip is a k -flip. In this case, the flipped pair is k -crossing (Lemma 4.2). We have the following inequality by definition of a k -flip: $i_1 \leq k \leq i_2$. There are three sub-cases.

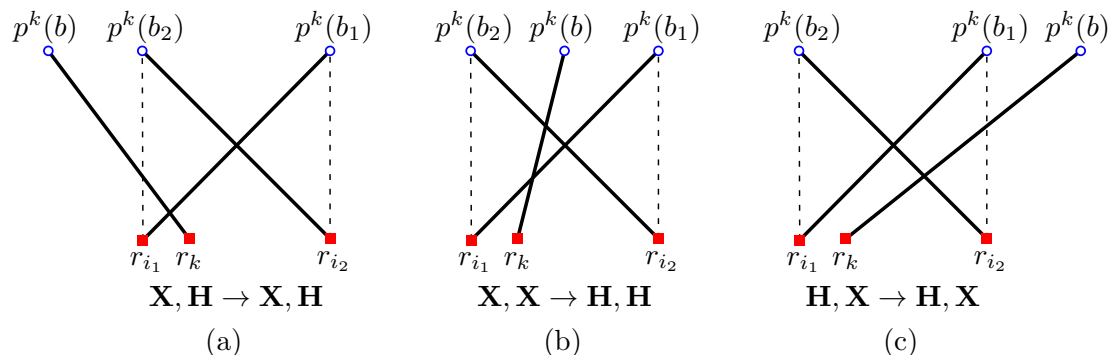


Figure 20: Cases 1.1.

Case 1.1: the flip is a k -flip, and $i = k$. Figure 20 displays the three sub-cases (a), (b) and (c). In case 1.1(a), statement (3) is not empty and holds. In case 1.1(b), all the statements (1), (2), (3), and (4) are empty. Case 1.1(c) is symmetric to case 1.1(a).

Case 1.2: the flip is a k -flip, $i \neq k$, and $i \in]i_1, i_2[$. Without loss of generality, we assume $k < i < i_2$. Figure 21 displays the three sub-cases (a), (b) and (c). In cases 1.2(a) and 1.2(b), all the statements (1), (2), (3), and (4) are empty. In case 1.2(c), statement (1) is not empty and holds.

Case 1.3: the flip is a k -flip, and $i \notin [i_1, i_2]$. Without loss of generality, we assume $i_2 < i$. Figure 22 displays the three sub-cases (a), (b), and (c). In cases 1.3(a) and 1.3(b), all the statements (1), (2), (3), and (4) are empty. In case 1.3(c), statement (1) is not empty and holds.

Case 2: the flip is not a k -flip. In this case, exactly one of the following inequalities holds: $i \leq k < i_1 < i_2$ or $i_1 < i_2 < k \leq i$. Without loss of generality, we suppose that the last inequality is the one to hold. Note that the flipped pair is not necessarily k -crossing, so the flip may look like a reverse flip after the projection p^k has been applied to the blue points. For example, in Figure 18, the crossing pair involving the red points r_1 and r_2 is not k -crossing, whereas the

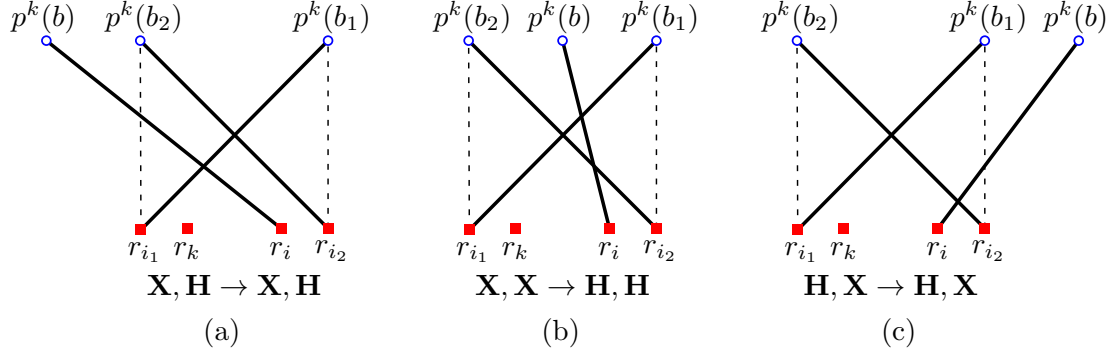


Figure 21: Cases 1.2.

crossing pair involving the red points r_4 and r_5 is k -crossing. Thus, there are two sub-cases, as follows.

Case 2.1: the flip is not a k -flip and the flipped pair is k -crossing. Figure 23 displays the three sub-cases (a), (b) and (c). In case 2.1(a), all the statements (1), (2), (3), and (4) are empty. In case 2.1(b), statement (3) is not empty and holds. In case 2.1(c), statement (4) is not empty and holds.

Case 2.2: the flip is not a k -flip and the flipped pair is not k -crossing. Figure 24 displays the three sub-cases (a), (b) and (c). In case 2.2(a), all the statements (1), (2), (3), and (4) are empty. In case 2.2(b), statement (3) is not empty and holds. In case 2.2(c), statement (4) is not empty and holds.

Lemma 4.4 follows from the four statements (1), (2), (3), and (4), proven true in all the fifteen cases. \square

We are now ready to define $\Phi(M)$, the *potential* of M , as the sum of $\Phi^k(M)$, for k in $\{1, \dots, n\}$. The following lemma presents the key properties of the potential Φ .

Lemma 4.5. *The potential Φ takes integer values from 0 to $\binom{n}{2} \frac{n+4}{3}$, and decreases of at least 2 units at each flip.*

Proof. We know that Φ takes non-negative integer values by definition.

Besides, by Lemma 4.3, the maximum of Φ is given by the following sum.

$$\sum_{k=1}^n (-k^2 + k(n+1) - 1) = \binom{n}{2} \frac{n+4}{3}$$

Finally, Φ decreases of at least 2 units at each flip because a flip of a pair $\{i, j\}$ is counted at least twice: once in Φ^i as an i -flip, and once in Φ^j as a j -flip. \square

Theorem 4.1 follows from Lemma 4.5.

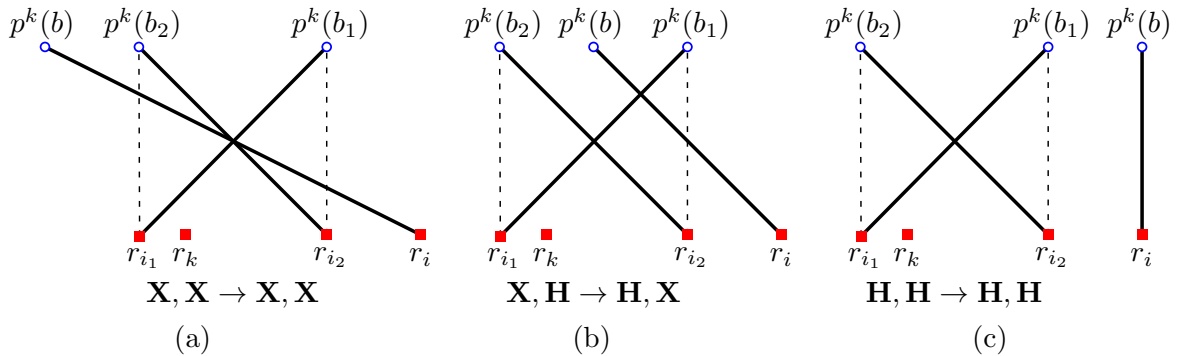


Figure 22: Cases 1.3.

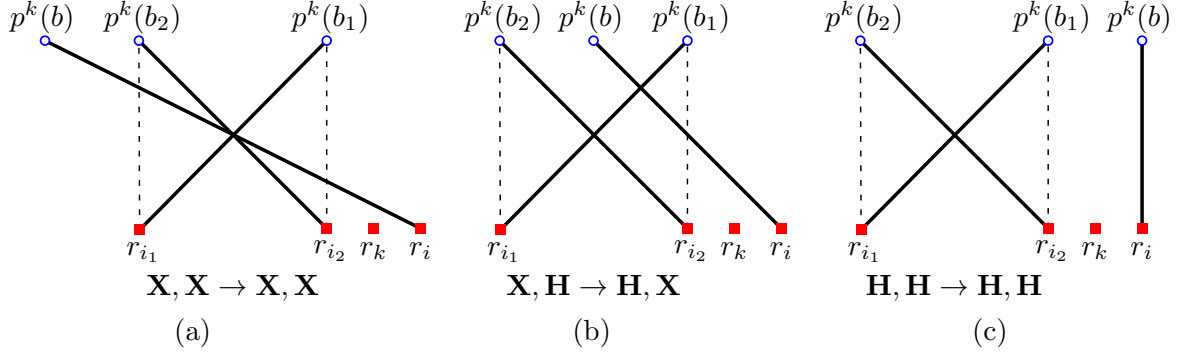


Figure 23: Cases 2.1.

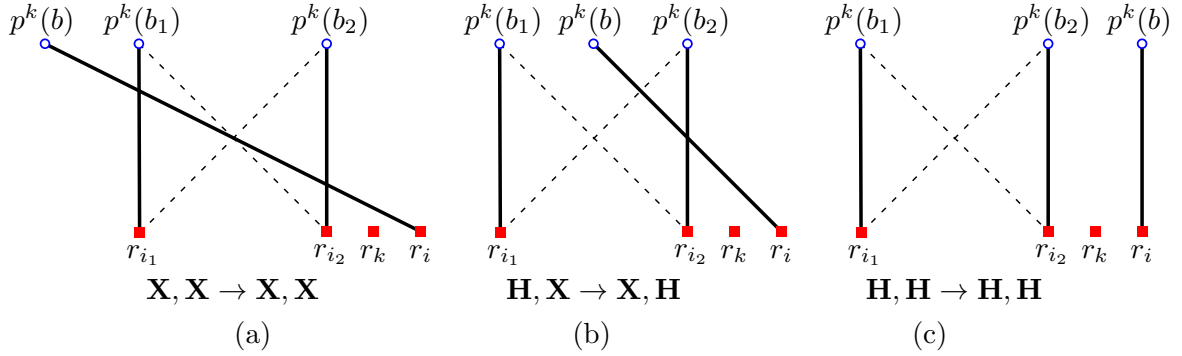


Figure 24: Cases 2.2.

5 Lower Bounds

In this section, we prove the following lower bounds.

Theorem 5.1. *In the red-on-a-line case, for even n , $\mathbf{D}(n) \geq \frac{3}{2} \binom{n}{2} - \frac{n}{4}$.*

Theorem 5.2. *In the convex case, for n multiple of 20, $\mathbf{d}(n) \geq 1.4 \cdot n$.*

5.1 Lower Bound on $D(n)$

In order to define the starting configurations of lower bounding untangle sequences, we first provide some ad hoc definitions. We call a red-on-a-line convex matching an n -star when the maximum crossing number is attained, i.e. all the $\binom{n}{2}$ pairs of segments are crossing. For convenience, we say an n -star *looks* at a point p if its blue points are all on a common line, and if p is the intersection of this line with the line on which the red points lay. We also say that two red-blue point sets R, B and R', B' are *fully crossing* if all the pairs of segments of the form $rb, r'b'$ are crossing, where $(r, b, r', b') \in R \times B \times R' \times B'$. Two matchings are fully crossing if their underlying red-blue point sets are fully crossing.

We define an m -butterfly as the red-on-a-line matching consisting of two fully crossing m -stars both looking at the same point p , where p is a median of the $2m$ red points (Figure 25).

We now prove Theorem 5.1 with two lemmas, showing that there exists an untangle sequence of length $\frac{3}{2} \binom{2m}{2} - \frac{m}{2}$ flips, starting at an m -butterfly.

Lemma 5.3 ([6]). *There exists an untangle sequence starting at any n -star of length $\binom{n}{2}$.*

Proof. Provided we number from 1 to n the red points in their convex hull counter-clock-wise order, and do the same for the blue points but clock-wise, then a red-on-a-line convex matching can be seen as a way to draw a permutation of n elements. An inversion, then, corresponds to a crossing. A bubble sort, thus, corresponds to an untangle sequence starting at such a matching.

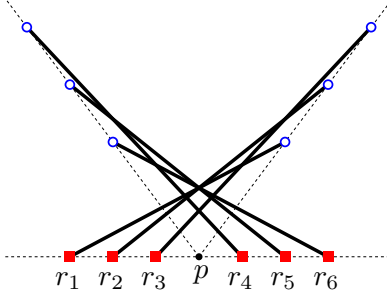


Figure 25: The 3-butterfly used to lower bound $\mathbf{D}(6)$.

The case of an n -star leads to $\binom{n}{2}$ inversion swaps, or, in other words, flips. \square

Lemma 5.4. *There exists an untangle sequence starting at any m -butterfly of length $\frac{3}{2}\binom{2m}{2} - \frac{m}{2}$ (Figure 27).*

Proof. We first number from left to right the $2m$ red points. The untangle sequence can be divided into two phases.

The first phase consists of (i) $\binom{m}{2}$ flips applied to the m -star submatching defined by the m leftmost red points (see Lemma 5.3, and Figure 27, steps 0 to 3), and of (ii) $\binom{m}{2}$ more flips applied to the m rightmost red points (steps 3 to 6). At this point, we have two sets of m “parallel” segments, each set fully crossing the other.

The second phase repeats m times the following routine.

1. Flip the segments defined by the innermost red points r_m and r_{m+1} (steps 6 to 7, 11 to 12, and 16 to 17).
2. Once again untangle the submatching defined by the m leftmost red points. It is well known [6] that there is an untangle sequence of length $m - 1$ from this submatching (steps 7 to 9, 12 to 14, and 17 to 19).
3. Symmetrically untangle the m rightmost red points with $m - 1$ more flips (steps 9 to 11, 14 to 16, and 19 to 21).

Each loop decreases the number of “long” segments (i.e. segments joining one of the leftmost red points to one of the rightmost blue points, or vice-versa) by 2. At the end of the process, the left submatching is crossing-free; so is the right one; and the two of them do not intersect anymore.

Summing up, the total number of flips is $2\binom{m}{2} + 2m(m - 1) + m$. Simple calculation yields the lemma. \square

Theorem 5.1 follows from Lemma 5.4.

As a final note, such counter-examples were found using flip expansion (i.e. replacing one flip generating two non-flip $\mathbf{X} \rightarrow \mathbf{H}$ transitions by three flips) on a loop scenario (i.e. when a column has no choice but to include a subsequence of transitions of the form $\mathbf{X} \rightarrow \mathbf{H} \rightarrow \mathbf{T} \rightarrow \mathbf{X} \rightarrow \mathbf{H}$) from state tracking (see Section 3).

5.2 Lower Bound on $d(n)$

An improved lower bound to $d(n)$ in the convex case comes from running a breadth-first search on the 20-segment configuration in Figure 26 and finding a minimum untangle sequence length of 24. Arranging multiple copies of this configuration, we get $d(n) \geq 1.4 \cdot n$ for n multiple of 20. The source code is available on github.com/gfonsecabr/untangling.

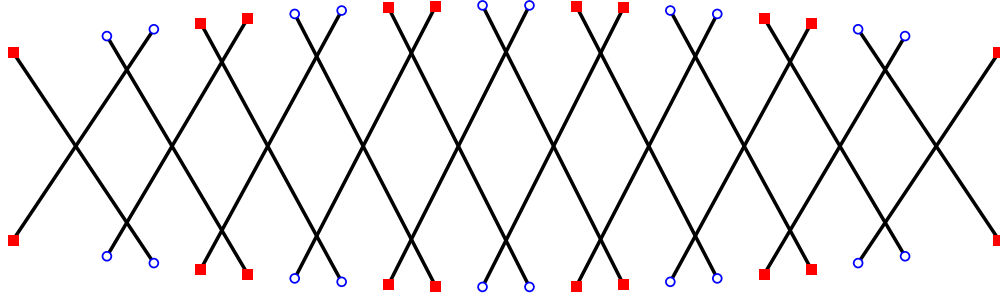


Figure 26: The convex configuration used to show that $d(20) \geq 28$.

References

- [1] Oswin Aichholzer, Wolfgang Mulzer, and Alexander Pilz. Flip distance between triangulations of a simple polygon is NP-complete. *Discrete & computational geometry*, 54(2):368–389, 2015.
- [2] Sergey Bereg and Hiro Ito. Transforming graphs with the same degree sequence. In *Computational Geometry and Graph Theory*, pages 25–32, 2008.
- [3] Sergey Bereg and Hiro Ito. Transforming graphs with the same graphic sequence. *Journal of Information Processing*, 25:627–633, 2017.
- [4] Ahmad Biniaz, Anil Maheshwari, and Michiel Smid. Flip distance to some plane configurations. *Computational Geometry*, 81:12–21, 2019.
- [5] Marthe Bonamy, Nicolas Bousquet, Marc Heinrich, Takehiro Ito, Yusuke Kobayashi, Arnaud Mary, Moritz Mühlenhaller, and Kunihiro Wasa. The perfect matching reconfiguration problem. *CoRR*, abs/1904.06184, 2019. [arXiv:1904.06184](https://arxiv.org/abs/1904.06184).
- [6] Édouard Bonnet and Tillmann Miltzow. Flip distance to a non-crossing perfect matching. *arXiv preprint arXiv:1601.05989*, 2016.
- [7] Prosenjit Bose and Ferran Hurtado. Flips in planar graphs. *Computational Geometry*, 42(1):60–80, 2009.
- [8] Nicolas Bousquet and Alice Joffard. Approximating shortest connected graph transformation for trees. In *Theory and Practice of Computer Science (SOFSEM 2020)*, pages 76–87, 2020.
- [9] Mark De Berg and Amirali Khosravi. Optimal binary space partitions for segments in the plane. *International Journal of Computational Geometry & Applications*, 22(03):187–205, 2012.
- [10] Matthias Englert, Heiko Röglin, and Berthold Vöcking. Worst case and probabilistic analysis of the 2-Opt algorithm for the TSP. *Algorithmica*, 68(1):190–264, 2014.
- [11] Péter L Erdős, Zoltán Király, and István Miklós. On the swap-distances of different realizations of a graphical degree sequence. *Combinatorics, Probability and Computing*, 22(3):366–383, 2013.
- [12] Seifollah Louis Hakimi. On realizability of a set of integers as degrees of the vertices of a linear graph. i. *Journal of the Society for Industrial and Applied Mathematics*, 10(3):496–506, 1962.

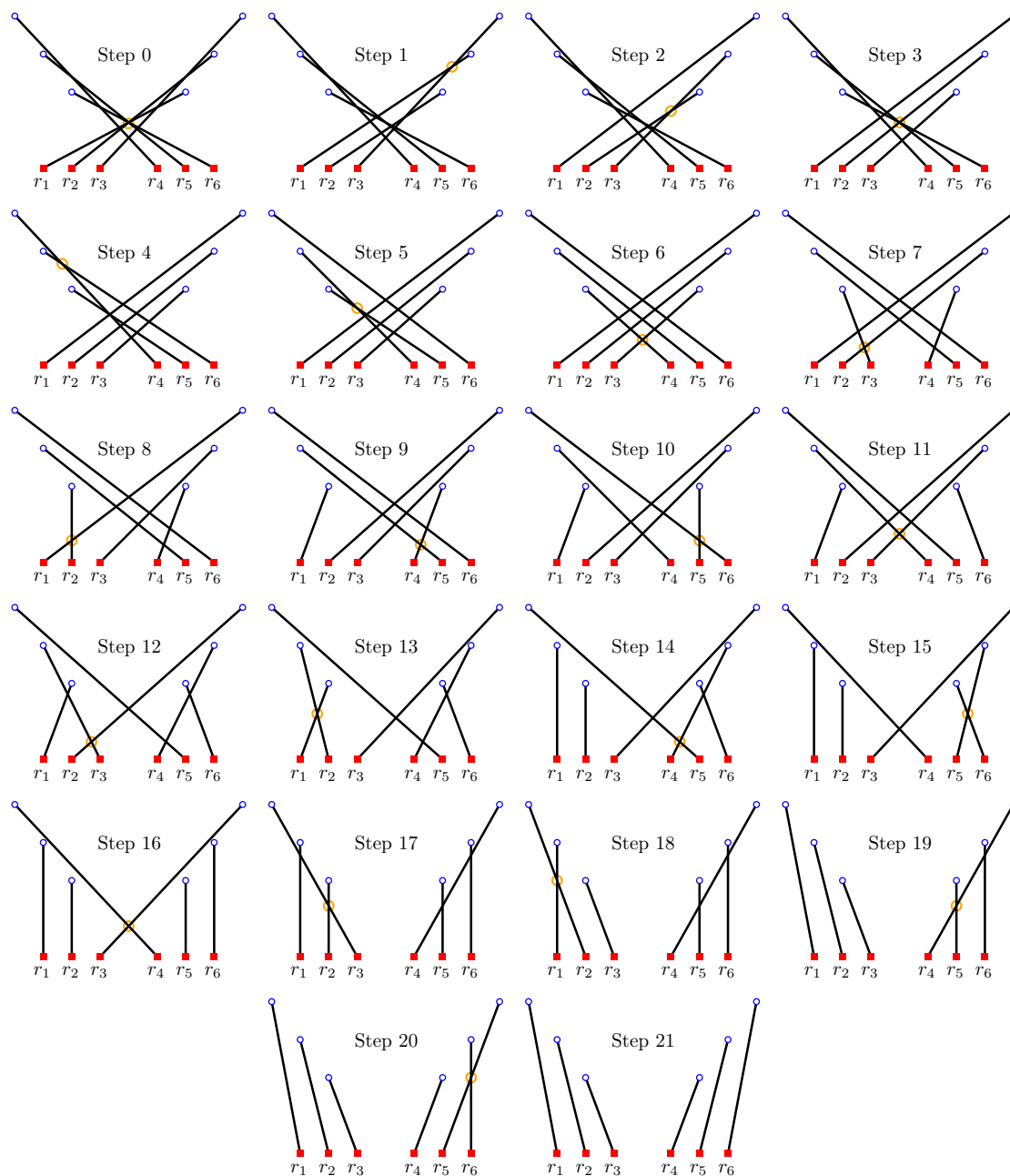


Figure 27: Untangle sequence starting at a 3-butterfly of length 21. The next flip is circled.

- [13] Seifollah Louis Hakimi. On realizability of a set of integers as degrees of the vertices of a linear graph ii. uniqueness. *Journal of the Society for Industrial and Applied Mathematics*, 11(1):135–147, 1963.
- [14] Ferran Hurtado, Marc Noy, and Jorge Urrutia. Flipping edges in triangulations. *Discrete & Computational Geometry*, 22(3):333–346, 1999.
- [15] Takehiro Ito, Erik D. Demaine, Nicholas J.A. Harvey, Christos H. Papadimitriou, Martha Sideri, Ryuhei Uehara, and Yushi Uno. On the complexity of reconfiguration problems. *Theoretical Computer Science*, 412(12):1054–1065, 2011.
- [16] Alice Joffard. *Graph domination and reconfiguration problems*. PhD thesis, Université Claude Bernard Lyon 1, 2020.
- [17] Charles L Lawson. Transforming triangulations. *Discrete mathematics*, 3(4):365–372, 1972.
- [18] Anna Lubiw and Vinayak Pathak. Flip distance between two triangulations of a point set is NP-complete. *Computational Geometry*, 49:17–23, 2015.
- [19] Naomi Nishimura. Introduction to reconfiguration. *Algorithms*, 11(4), 2018.
- [20] Yoshiaki Oda and Mamoru Watanabe. The number of flips required to obtain non-crossing convex cycles. In *Kyoto International Conference on Computational Geometry and Graph Theory*, pages 155–165, 2007.
- [21] Alexander Pilz. Flip distance between triangulations of a planar point set is apx-hard. *Computational Geometry*, 47(5):589–604, 2014.
- [22] Jan van den Heuvel. The complexity of change. *CoRR*, abs/1312.2816, 2013. [arXiv:1312.2816](https://arxiv.org/abs/1312.2816).
- [23] Jan van Leeuwen. Untangling a traveling salesman tour in the plane. In *7th Workshop on Graph-Theoretic Concepts in Computer Science (WG 1981)*, 1981.
- [24] Todd G Will. Switching distance between graphs with the same degrees. *SIAM Journal on Discrete Mathematics*, 12(3):298–306, 1999.
- [25] David P. Williamson and David B. Shmoys. *The Design of Approximation Algorithms*. Cambridge University Press, USA, 1st edition, 2011.
- [26] Ro-Yu Wu, Jou-Ming Chang, and Jia-Huei Lin. On the maximum switching number to obtain non-crossing convex cycles. In *26th Workshop on Combinatorial Mathematics and Computation Theory*, pages 266–273, 2009.